Michigan State University

National Superconducting Cyclotron Laboratory

FRAGMENTATION OF ^{78}Kr PROJECTILES

R. PFAFF, D.J. MORRISSEY, W. BENENSON, M. FAUERBACH, M. HELLSTRÖM, C.F. POWELL, B.M. SHERRILL, M. STEINER, and J.A. WINGER

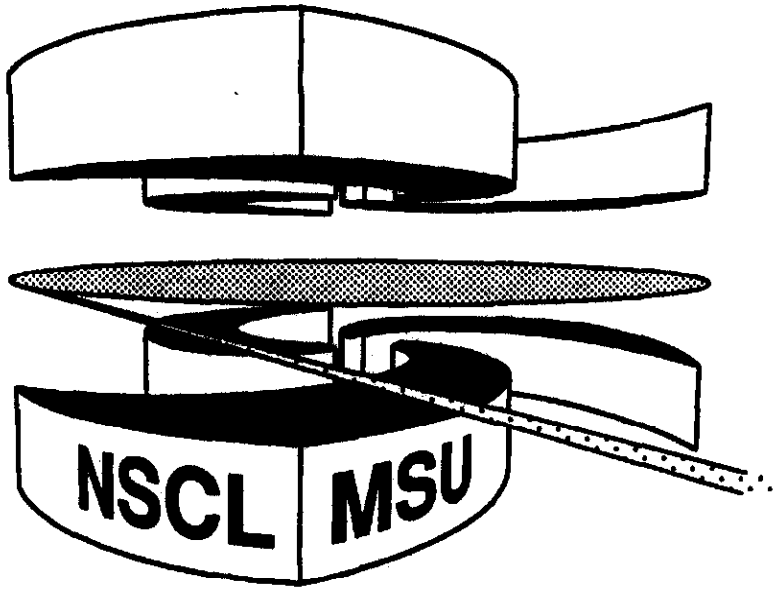

MSUCL-1006 **JANUARY 1996**

Fragmentation of ^{78}Kr projectiles

R. Pfaff[1,2], D.J. Morrissey [2,3], W. Benenson[1,2], M. Fauerbach[1,2], M. Hellström[2,*], C. F. Powell[2,3], B.M. Sherrill[1,2], M. Steiner',', and J.A. Winger[4]

[1]*Department of Physics and Astronomy, Michigan State* University, *East Lansing, MI 48824*

[2]*National* Superconducting *Cyclotron Laboratory, Michigan State University, East Lansing, MI 48824*

[3]*Department of Chemistry, Michigan State University, East Lansing, MI 48824*

[4]*Department of Physics and Astronomy, Mississippi State University, Mississippi State, MS 39762*

Abstract

To gain a better understanding of the production of exotic isotopes and provide information on the stability of nuclei along the path of the rapid-proton capture process, isotopic cross sections from the reaction ^{78}Kr + ^{58}Ni at 75 MeV/nucleon were measured at 0° using the A1200 fragment separator. Most notably the particle stability of ^{69}Br was thoroughly probed during this experiment and it appears to be particle unstable. The experimental production cross section data are compared to previous krypton isotope fragmentation data to explore the dependence of the N/Z ratio of the projectile on the observed isotopic distributions ("memory effect") as well as with an intranuclear cascade code developed for higher energies (> 200 MeV/nucleon) and a semiempirical parameterization derived from high energy systematics.

25.70.Mn, 21.10.Tg, 27.50.+e

I. INTRODUCTION

Projectile fragmentation has proven to be an important tool for producing nuclei very far from stability. Use of this process has led to progress in many current research areas including the location of possible termination points of the rapid-proton capture process (rp-process) and the study of the memory effect caused by projectiles with different N/Z ratios. The rp-process was first proposed by Wallace and Woosley [1] and showed that heavy isotopes (up to A=100) could be produced in astrophysical processes in which high temperatures and densities exist, such as supernova shock waves, novae, and x-ray bursts [2,3]. The rp-process proceeds via a sequence of proton capture and β^+ decays near and sometimes along the proton drip line. Particle stability and half-lives are important in determining the rate and actual path of the rp-process since it occurs during explosive processes in short time periods ($\sim$ 10 - 100 sec). When the rp-process path must pass through isotopes with long β^+ half-lives, the rp-process will be slowed or terminated. Mass models [4] differ on predictions of the exact position of the proton drip line which prompted several experiments that looked for possible termination points of the rp-process [5,6]. In recent years the odd Z isotopes of ^{65}As and ^{69}Br have been investigated as the most likely termination points because the half-lives of ^{64}Ge and ^{68}Se, the proton capture targets, are thought to be longer than the time scale of the explosion that provides the proton flux.

Evidence for the existence of ^{65}As and ^{69}Br (along with four other new isotopes) was first reported by Mohar *et al.* [6]. A subsequent experiment measured the half-life of several of the isotopes including ^{65}As; however, ^{69}Br was not observed [7,8]. A recent experiment at GANIL [9] reported five new isotopes (^{60}Ga, ^{64}As, ^{69,70}Kr, and ^{74}Sr) which extended the experimentally observed proton drip line, but no events were attributed to ^{69}Br. The latter experiment had a flight path six times longer than the one in Ref. [6], indicating that ^{69}Br was not stable or had a very short half life ($<$ 100 ns). To explore these possibilities a new experiment was performed using the A1200 device [10] at the National Superconducting Cyclotron Laboratory (NSCL) that would be sensitive to nuclei with such very short ($\sim$ 100

ns) half-lives.

The present study of the proton-drip line nuclei involved the measurement of production cross sections of many proton-rich isotopes, thus allowing a parallel investigation of the so-called "memory" effect [11]. Fragmentation is generally described as a two step process in which the projectile will rapidly interact with the target, producing excited "prefragments". These then undergo a slower de-excitation step via sequential evaporation of particles, finally producing the observed reaction residues ("fragments"). Prefragments with (very) high excitation energies are likely to produce final products along a ridge parallel to the valley of β stability (e.g. Ref. [12]), and thus fragments far from the projectile will have no "memory" of the N/Z ratio of the projectile. It is, however, well-known that if the projectile has a *high* N/Z ratio (i.e., is neutron rich), especially those prefragments that are close to the projectile mass have many loosely bound neutrons that even at low excitation energies will be preferentially (relative to protons) evaporated, resulting in observed fragments with a lower N/Z ratio than that of the projectile.

On the other hand, the projectile-like prefragments (particularly those with low excitation energies) produced from a projectile with a *low* N/Z ratio (proton rich) are likely to evaporate both protons and neutrons, producing fragments that are relatively proton-rich, as was the projectile. Isotopic cross sections from fragmentation reactions involving members from both extremes of an isotopic chain can therefore provide crucial information on this influence of the projectile N/Z ratio on the fragment charge dispersion distribution ("memory effect"). Data from the current experiment, which utilized the very proton-rich ^{78}Kr projectile (N/Z $\sim$ 1.17) are compared to data from earlier experiments [12,13] that involved fragmentation of the very neutron-rich krypton isotopes ^{86}Kr (N/Z $\sim$ 1.39) and ^{84}Kr (N/Z $\sim$ 1.33).

II. EXPERIMENTAL PROCEDURE

A 75 MeV/nucleon ^{78}Kr beam ($\sim$ 45 particle pA) impinged on a 102 mg/cm^2 ^{58}Ni target placed in the mid-acceptance target position of the recently upgraded A1200 fragment separator [8,10] at the National Superconducting Cyclotron Laboratory (NSCL). The angular acceptance for fragments was $\Delta\theta$ = 20 mrad and $\Delta\phi$ = 40 mrad centered around 0° with a momentum acceptance of $\pm$1.5%. The magnetic rigidity was varied in overlapping steps which covered the range in Bρ from 2.274 to 2.488 Tm. The normalization between the different rigidity settings was obtained by comparison of the isotopic yields in the regions of overlapping rigidity. The fragments were stopped in a silicon telescope located at the focal plane of the A1200 or, to observe a possible short half-life that might explain the discrepancy between previous experiments [6,9], in a second silicon telescope located 7.5 m further downstream from the focal plane. (Note that for isotopes with half-lives on the order of $\sim$ 100 ns, a reduced isotopic count rate would be observed in the second silicon telescope relative to the first.)

The time of flight (TOF) of the reaction products was measured between a 8 mg/cm^2 plastic scintillator at the first dispersive image position and the frontmost detector in each silicon telescope, with flight paths of 14 m and 21.5 m, respectively. The position and angle of the reaction products was measured at both the second dispersive image and the focal plane with pairs of parallel-plate avalanche counters (PPACs) [14] separated by 40 cm. The position information at the second dispersive image together with NMR measurements of the A1200 dipole fields enabled the momentum of each particle to be determined. The reaction products were implanted into either of the two four-element silicon telescopes, each consisting of two thin ΔE detectors followed by two thick E detectors (100 μm, 75 μm, 500 μm, and 1000 μm). All the silicon detectors had an active area of 300 mm^2. Due to the excellent energy and time resolution, the online identification using ΔE vs. TOF diagrams, an example of which is shown in Fig. 1, was carried out in a straightforward manner. Using the values of ΔE, total kinetic energy, TOF, and magnetic rigidity, the mass (A), proton

number (Z), and charge (Q) of each particle were determined using the procedure described in Ref. [13].

The parallel momentum distributions of a number of reaction products were monitored online and fitted with a Gaussian function. The centroid values were then used to identify the most appropriate magnetic rigidity setting for the observation of ^{69}Br. The centroids (in terms of magnetic rigidity) for the isotopes covering Z = 24 to 38 are shown in Fig. 2 where the horizontal dashed lines show the range of magnetic rigidity covered during this experiment. The general trends exhibited by the reaction products and in particular that of the bromine isotopes, show that this rigidity range would have allowed for observation of ^{69}Br.

III. RESULTS AND DISCUSSION

A. Isotopic yields

Figure 3 shows the mass spectra for isotopes with atomic numbers $30 \leq Z \leq 38$ obtained at a fixed magnetic rigidity setting optimized for observation of ^{69}Br. The absence of ^{69}Br is clearly observed in the bromine mass spectrum, whereas other T_z = -1/2 nuclei are present. The asterisk symbols in Fig. 3 indicate several events that can be attributed to ^{60}Ga and ^{70}Kr, confirming the recent identification of these isotopes by Blank *et al.* [9]. The measured isotopic cross sections, determined by integrating the Gaussian functions over momentum space after correcting for the acceptance of the A1200, are shown in Fig. 4.

Also shown in Fig. 4 are the cross sections calculated from both the EPAX parameterization [15] and the ISApace model [16]. Both codes were originally developed for high energy (or "pure") fragmentation (E/A > 200 MeV/nucleon), but recent experiments have shown their applicability for reactions involving intermediate-mass projectiles at intermediate energies [13,17]. A comparison of the (absolute) experimental cross sections with the EPAX parameterization and the ISApace code shows several overall features. The EPAX code no-

ticeably underpredicts the formation of proton pick-up products (Z > 36), a not unexpected feature considering this parameterization was developed from high-energy fragmentation in which pick-up reactions seldom occur. The ISApace code is able to relatively well reproduce the single-proton pick-up, but the predicted cross sections for reaction products that have acquired more than one proton (Z > 37) start to fall off dramatically. The magnitude of the predicted cross sections from both EPAX and ISApace agree relatively well for the reaction products below krypton (Z < 36), although the predicted distributions are more neutron-rich than the experimental cross section distributions (Z $\geq$ 30).

B. Implications for the rp-process

From the isotopic cross sections shown in Fig. 4, it is possible to estimate the number of ^{69}Br events that should have been observed. Assuming an exponential decrease in cross section near the proton drip line (as is predicted by the EPAX parameterization [15]), $\sim$ 300 counts of ^{69}Br should have been observed given the number of ^{70}Br events that were identified. This estimated number of events that should have been observed can, together with the short flight path ($\sim$14 m from production target to the focal plane silicon telescope), be used to place an upper limit on the half-life of ^{69}Br of 24 ns. Most mass models predict ^{69}Br to be only slightly proton unbound. In the 1993 Atomic Mass Tables [18] the value of S_p= -180 $\pm$ 300 keV is found from the listed binding energies of ^{69}Br and ^{68}Se. Assuming that the proton is emitted from a $p_{\frac{1}{2}}$ state (as is the case in the mirror nucleus ^{69}Se), the proton penetrability WKB approximation indicates a half-life of $\sim 10^3$ seconds which implies that the main decay mode is β^+/EC with an estimated half-life on the order of 100 ms [19]. For the WKB approximation a normalized Wood-Saxon nuclear potential was used in conjunction with the centrifugal, spin-orbit, and Coulomb terms as was described Ref. [7]. The recent GANIL experiment [9] limited the ^{69}Br half-life to 100 ns or less which corresponds to being proton unbound by at least 450 keV. The current tighter limit on the ^{69}Br half-life of 24 ns or less indicates that this nucleus is proton unbound by at least 500

keV.

The present experiment also gives some information on ^{73}Rb. Because of its non-observation in a wide variety of measurements over a number of years [6,9,20,21], this isotope is generally thought to be particle unbound. The systematics in Fig. 2 show that the magnetic rigidity range covered in the present experiment would also have included ^{73}Rb. Using the EPAX parameterization and the observed number of ^{74}Rb events, approximately 75 ^{73}Rb events should have been observed, yielding an effective upper limit of 30 ns for the half-life of ^{73}Rb. In the case of ^{73}Rb, the majority of mass models predict this isotope to be proton unbound. The value of S_p = -590 $\pm$ 270 keV determined from binding energies in the 1993 Atomic Mass Tables [18] yields a proton emission half-life of $\sim$ 700 ns (using the WKB approximation). The present data limits the half-life of ^{73}Rb to less than 30 ns and assuming the emitted proton comes from the $f_{\frac{5}{2}}$ state (since the mirror nucleus is ^{73}Kr) indicates that ^{73}Rb is unbound by at least 680 keV.

Under the previous assumption that ^{69}Br was particle stable [3], the rp-process was generally thought to proceed via

$$^{68}\mathrm{Se(p,\gamma)}^{69}\mathrm{Br}(\beta^+)^{70}\mathrm{Kr}(\beta^+)^{70}\mathrm{Br(p,\gamma)}^{71}\mathrm{Kr}(\beta^+)^{71}\mathrm{Br(p,\gamma)}^{72}\mathrm{Kr}.$$

In view of their recent results (regarding the particle instability of ^{69}Br), Blank *et al.* [9] have proposed an alternative rp-process path:

$$^{68}\mathrm{Se}(\beta^+)^{68}\mathrm{As(p,\gamma)}^{69}\mathrm{Se(p,\gamma)}^{70}\mathrm{Br(p,\gamma)}^{71}\mathrm{Kr}(\beta^+)^{71}\mathrm{Br(p,\gamma)}^{72}\mathrm{Kr}.$$

The most significant modification is that the rp-process must now wait for the decay of ^{68}Se which has a long half-life (1.6 min) relative to the assumed burning time ($\sim$ 10 sec) of the astrophysical processes in which the rp-process is likely to proceed to the high mass region (A > 70). boron) In processes with extended burning times ($\sim$ 100 sec) [2,3], the rp-process can slowly continue to ^{72}Kr which slows the process due to the fact that ^{73}Rb is unstable and ^{72}Kr has a 17.2 second half-life. Many of the rp-process calculations [2,3] are extended to $\sim$ 1000 seconds to explore the astrophysical effects of an extended burning time and in this situation the rp-process could slowly proceed to masses higher than ^{72}Kr.

Of the five new isotopes reported by Blank *et al.* [9], two (^{60}Ga and ^{64}As) could alter the rp-process path as it approaches ^{68}Se. The other three isotopes (of ^{69}Kr, ^{70}Kr, and ^{74}Sr), however, have no influence on the modified rp-path due to the "bottle-necks" caused by the instability of ^{69}Br and ^{73}Rb. Although no evidence for ^{64}As, ^{69}Kr, and ^{74}Sr was seen in the present experiment (assuming an exponential decrease in cross section and the number of events attributed to ^{65}As, ^{70}Kr, and ^{75}Sr, no counts of ^{64}As, ^{69}Kr, and ^{74}Sr should have been observed), the modified rp-process path presented by Blank *et al.* [9] seems to accurately reflect the current experimental evidence.

C. Memory Effect

Together with the results of previous experiments involving fragmentation of neutron-rich krypton projectiles (^{86}Kr [13] and ^{84}Kr [12]), the data from the present experiment can provide additional insight into the influence of the projectile N/Z ratio on the fragment charge dispersion distribution for reactions in the intermediate energy/intermediate mass regime. In order to properly include this effect into their semi-empirical fragmentation product cross section code, Sümmerer *et al.* [15] developed a parameterization that took into account previous observations from (target) fragmentation experiments; (i) the maxima of fragment charge distributions always lie on the neutron-deficient side of the valley of β stability, (ii) for targets/projectiles close to β-stability, the most probable charge of a fragment isobaric chain is only dependent on fragment mass, and (iii) the size of the memory effect is different for neutron- and proton-rich projectiles. Chu *et al.* [11] had described this effect as

$$Z_p(A) = Z_\beta(A) + \Delta \tag{1}$$

where $Z_p(A)$ is the most probable charge and the β-stable charge $Z_\beta(A)$ can be approximated by the smooth function (thus avoiding shell effects) [22]

$$Z_\beta(A) = \frac{A}{1.98 + 0.0155 \cdot A^{\frac{2}{3}}}. \tag{2}$$

The Δ term, which describes the difference between experimentally obtained values of Z_p and Z_β, was parameterized by Sümmerer *et al.* [15] using the form

$$\Delta = \begin{cases} 2.041\text{x}10^{-4} \cdot \text{A}^2 & \text{if A} < 66 \\ 2.703\text{x}10^{-2} \cdot \text{A} - 0.895 & \text{if A} \geq 66 \end{cases} \quad (3)$$

To describe the additional shift in the charge distribution maxima (Z_p) that is caused by the N/Z ratio of the target/projectile (depending on whether target- or projectile-like residues are studied) an extra "memory effect" term Δ_m was added:

$$Z_p(A) = Z_\beta(A) + \Delta + \Delta_m. \quad (4)$$

A fit to the (scarce) experimental data available at the time led to a parameterization for Δ_m in the form

$$\Delta_m(A) = \left[c_1 \left(\frac{A}{A_t}\right)^2 + c_2 \left(\frac{A}{A_t}\right)^4 \right] \Delta_\beta(A_t) \quad (5)$$

where A_t is the target mass and $\Delta_\beta(A_t) = Z_t - Z_\beta(A_t)$, in which Z_t is the target proton number and A_t is the target mass. Different values for the coefficients c_1 and c_2 were determined for neutron- and proton-rich fragmentation as the memory effect appeared to be smaller for fragmentation of proton-rich targets/projectiles compared to neutron-rich systems.

Figure 5 illustrates the dependence of the memory effect Δ_m on the ratio of A_f/A_p (where A_f is the fragment mass and A_p is the projectile mass) for the most abundantly produced final fragment of each isobaric chain (the so-called "ridge line") from the present experiment. The ridge lines are shown also from two other experiments with more neutron-rich krypton isotopes: ^{86}Kr fragmentation at 70 MeV/nucleon [13] and ^{84}Kr fragmentation at 200 MeV/nucleon [12]. Also indicated in Fig. 5 is the curve representing the parameterization of Eq. 5 for the ^{78}Kr fragmentation (the parameterization for the reactions involving ^{84}Kr and ^{86}Kr are not shown on the plot, but exhibit similar agreement to the data as that for the ^{78}Kr fragmentation data). It is apparent that the memory effect for intermediate energy/intermediate mass fragmentation behaves differently than expected from the high

energy data. Both the data from the current proton-rich fragmentation of ^{78}Kr as well as the data from the neutron-rich fragmentation of ^{84}Kr and ^{86}Kr show a much steeper dependence on the mass ratio than the parameterization. Recent measurements with ^{129}Xe and ^{136}Xe beams at 790 MeV/nucleon showed a similar trend for the proton-rich projectile and the reaction products from the neutron-rich projectile (^{136}Xe) as they deviated from the standard parameterization [23]. Using the same formalism as Sümmerer *et al.* [15], the memory effect from the three intermediate-energy krypton fragmentation experiments can best be described by

$$\Delta_m = \left[c_1 \left(\frac{A}{A_p} \right)^4 + c_2 \left(\frac{A}{A_p} \right) \right] \Delta_\beta(A_p) \tag{6}$$

with values of c_1 = 1.55 and c_2 = -0.425. The modified parameterization was determined by performing a least square fit (with two n-th order polynomial terms) to the experimental data. The c_2 becomes negative to account for the fact that the proton-rich fragmentation data dips below the $\Delta_m = 0$ line (this effect was also observed in the limited data in Ref. [15]). The parameterization shows that fragments far from the projectile approach the valley of β stability ($\Delta_m/\Delta_\beta(A_t) \sim 0$) and those near the projectile mass are close to the N/Z ratio of the projectile ($\Delta_m/\Delta_\beta(A_t) \sim 1$). This modified parameterization does a good job reproducing the experimental data and is indicated by solid curves in Fig. 5. (Because the ^{86}Kr fragmentation experiment [13] was concentrated on fragments near the Z of the beam, this data is limited to Z $\geq$ 33.) It should also be noted that, in contrast to the two other data sets which were measured around 0°, the ^{84}Kr [12] data was obtained at angles of 0.6° and 1.5°. The fact that the ^{84}Kr ridge line in Fig. 5 begins to curve downward for Z < 20 indicates that parts of the parameterization used in this analysis are not applicable near and below argon (Z = 18), as was discussed by Sümmerer *et al.* [15].

Charge pick-up products (Z > 36 in this case), which are rarely produced from high energy fragmentation, are commonly observed at intermediate energies. The memory effects for the pick-up products observed in previous krypton fragmentation experiments [12,13], as indicated in Fig. 5 by unfilled symbols, seem to closely follow the general trend of

the fragmentation products ($Z \leq 36$). This fact, together with the observation that the overall curvature of the memory effect is steeper than the standard parameterization, is a strong indication that the prefragments are produced by processes other than the "pure" fragmentation that occur in high energy reactions. This assumption is also supported by the relatively large pick-up product cross sections that were observed in the current experiment and the ^{86}Kr fragmentation [13].

IV. CONCLUSIONS

The present experiment clearly indicates that ^{69}Br is proton unbound by at least 500 keV and thereby confirms the recent work of Blank *et al.* [9]. This result implies that the rp-process will be significantly slowed down at ^{68}Se, since the β-decay half life is very long relative to the timescales of the astrophysical processes in which the rp-process is thought to occur. Another significant rp-process "bottle-neck" occurs due the particle-instability of ^{73}Rb, for which the present experiment indicates that it is proton unbound by at least 680 keV. Of the five new isotopes recently reported by Blank *et al.* [9], ^{70}Kr and ^{60}Ga were observed during the current experiment. Blank *et al.* proposed a modified rp-path to reflect the recent experimental evidence of new isotopes and the particle instability of ^{69}Br. It is apparent that further research will be necessary to accurately describe the extent and rates of the rp-process reactions in this mass region. The present study of the memory effect in krypton fragmentation shows that the N/Z ratio of the projectile does have a significant impact on the isotopic distribution. Evidence from the current experiment along with that from other intermediate energy krypton fragmentation experiments [13,12] show that final fragment distributions near the beam (high A_f/A_p values) tend to be very neutron- or proton-rich (depending on the projectile) and show a rapid decay (as A_f/A_p decreases) towards the valley of β stability relative to the high-energy data that was used to develop the parameterization of Ref. [15]. energy data. This, together with the large cross sections observed for pick-up reactions gives clear evidence that other reaction processes than "pure"

fragmentation occur during interactions of intermediate mass nuclei at intermediate energies.

This work was supported by the National Science Foundation under Grant number PHY-92-14922.

REFERENCES

* Present address: Gesellschaft für Schwerionenforschung mbH, Postfach 11 05 52, D-64220 Darmstadt, Germany.

[1] R.K. Wallace and S.E. Woosley, Astrophys. J. Suppl. **45**, 389 (1981).

[2] L. Van Wormer, J. Görres, C. Iliadis, F.-K. Thielemann, and M. Wiescher, Astrophys. J. **432**, 326 (1994).

[3] A.E. Champagne and M. Wiescher, Annu. Rev. Nucl. Part. Sci. **42**, 39-76 (1992).

[4] J. Jänecke and P.J. Mason, At. Data Nucl. Data Tables **39**, 185 (1988).

[5] J.D. Robertson, J.E. Reiff, T.F. Lang, D.M. Moltz, and J. Cerney, Phys. Rev. C **42**, 1922 (1990).

[6] M.F. Mohar, D. Bazin, W. Benenson, D.J. Morrissey, N.A. Orr, B.M. Sherrill, D. Swan, and J.A. Winger, Phys. Rev. Lett. **66**, 1571 (1991).

[7] J.A. Winger *et al.*, Phys. Rev. C **48**, 3097 (1993).

[8] M. Hellström and D. J. Morrissey, Nucl. Instrum. Methods B **99**, 342 (1995).

[9] B. Blank *et al.*, Phys. Rev. Lett. **74**, 4611 (1995).

[10] B.M. Sherrill, D.J. Morrissey, J. A. Nolen Jr., and J A. Winger, Nucl. Instrum. Methods B **56**, 1106 (1991).

[11] Y.Y. Chu, E.M. Franz, G. Friedlander, and P.J. Karol, Phys. Rev. C **4**, 2202 (1971).

[12] C. Stéphan *et al.*, Phys. Lett. **262B**, 6 (1991).

[13] R. Pfaff *et al.*, Phys. Rev. C **51**, 1348 (1995).

[14] D. Swan, J. Yurkon, and D.J. Morrissey, Nucl. Instrum. Methods A **348**, 314 (1994).

[15] K. Sümmerer, W. Brüchle, D.J. Morrissey, M. Schädel, B. Szweryn, and Yang Weifan,

Phys. Rev. C **42**, 2546 (1990).

[16] M. Fauerbach, Diploma thesis, TH Darmstadt (1992).

[17] M. Fauerbach *et al.*, submitted to Phys. Rev. C.

[18] G. Audi and A.H. Wapstra, Nucl. Phys. A **565**, 1 (1993).

[19] K. Takahashi, M. Yamada, T. Kondoh, At. Data Nucl. Data Tables **12**, 101 (1973).

[20] J.M. D'Auria *et al.*, Phys. Rev. Lett. **66B**, 233 (1977).

[21] M. Hencheck *et al.*, Phys Rev. C **50**, 2219 (1994).

[22] P. Marmier and E. Sheldon, *Physics of Nuclei and Particles* (Academic, New York and London, 1971), Vol. I, p. 15.

[23] J. Friese, H.J. Körner, J. Reinhold, R. Schneider, K. Zeitelhack, H. Geissel, A. Magel, G. Münzenberg, K. Sümmerer, Proc. of the 3rd Int. Conf. on Radioactive Nuclear Beams (East Lansing, USA, May 1993), D.J. Morrissey, Ed., Edition Frontières (Gif-sur-Yvette, France, 1993)., pg. 333.

FIGURES

FIG. 1. The energy loss in the focal plane silicon telescope versus time-of-flight of the reaction products used for particle identification. Note the excellent resolution in both energy and time. The N=Z line and the krypton isotope band (Z=36) are indicated by dashed lines. The absence of ^{69}Br (expected position shown by arrow) is quite evident.

FIG. 2. Parallel momentum distribution centroids (in terms of magnetic rigidity (Tm)) versus atomic mass for reaction products with Z = 24 to 38. The projectile-like fragments exhibit the general trend expected from kinematics. The dashed horizontal lines indicate the rigidity region ($2.274 \leq B\rho \leq 2.488$ Tm) of the present study. The statistical error bars are shown when larger than the data symbols. The lines joining the isotopic chains are merely to guide the eye.

FIG. 3. Mass distributions for the isotopes of zinc (Z=30) through strontium (Z=38) recorded at a magnetic rigidity setting optimized for the observation of ^{69}Br. The asterisk symbols indicate the isotopes of ^{60}Ga and ^{70}Kr which were reported by Blank *et al.* [9]. The arrows show the absence of ^{69}Br and ^{73}Rb, two suggested termination points for the rp-process (due to the relatively long half-lives of ^{68}Se and ^{72}Kr.

FIG. 4. Isotopic cross sections for the elements between zinc and strontium from the reaction ^{78}Kr + ^{58}Ni at 75 MeV/nucleon. The solid points indicate the measured production cross sections. The dotted histograms represent the EPAX parameterization [15], while the solid histogram illustrates the cross sections calculated with the ISApace code [16]. The statistical error is generally smaller than the size of the data points.

FIG. 5. Parameterization of the "memory effect": the additional shift Δ_m, of the charge-dispersion curve is shown as a function of the fragment-to-projectile mass ratio. Positive values of Δ_m indicate a shift towards lower N/Z ratios (proton-rich). The isotopic ridge lines from the present experimental data and two previous experiments involving krypton fragmentation [12,13] are shown in the figure. The open symbols indicate charge pick-up products ($Z > 36$). The dashed curve indicates the parameterization of Sümmerer *et al.* [15] for the ^{78}Kr fragmentation (although not shown, the EPAX parameterization for the ^{84}Kr and ^{86}Kr fragmentation exhibit a similar trend relative to the respective data), while the solid curves represent the modified parameterization derived from the experimental krypton data as discussed in the text.

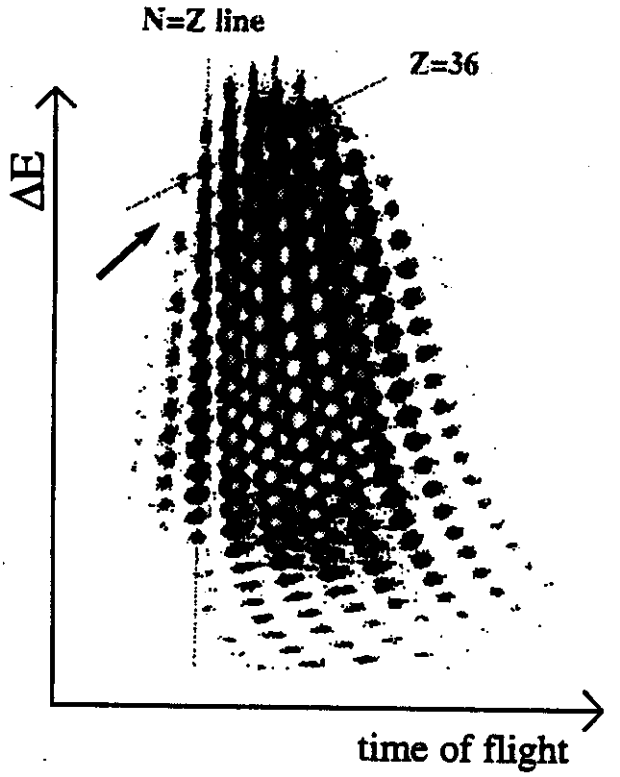

Figure 1

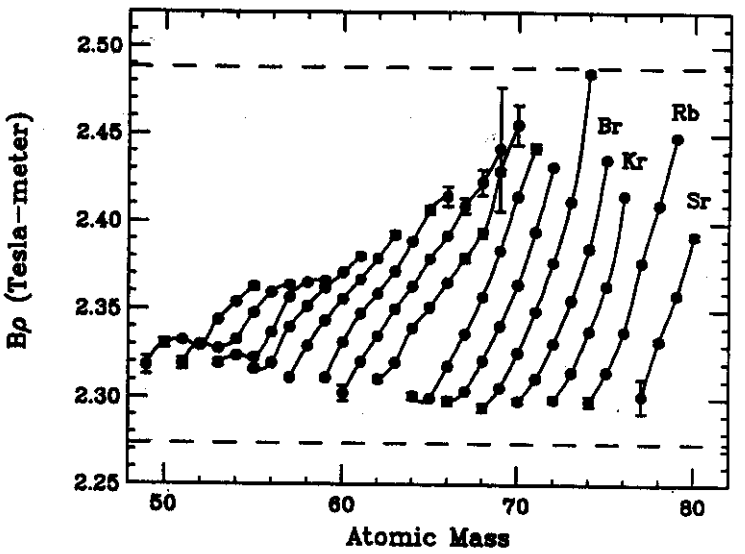

Figure 2

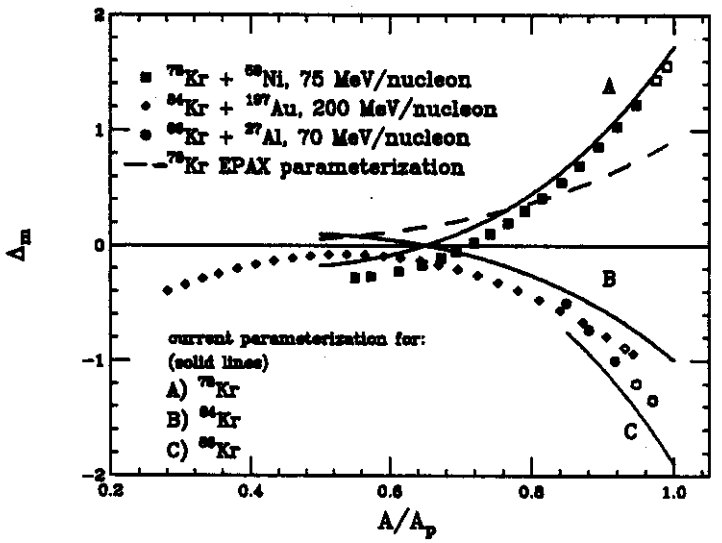

Figure 5

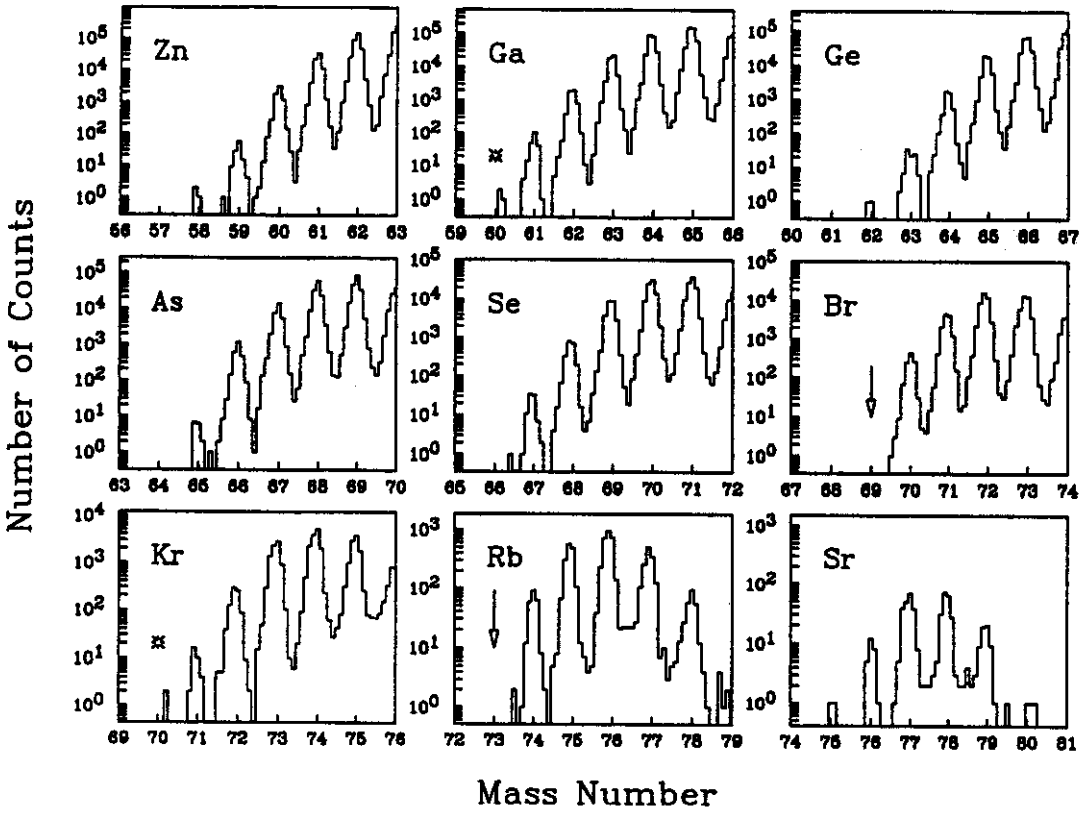

Figure 3

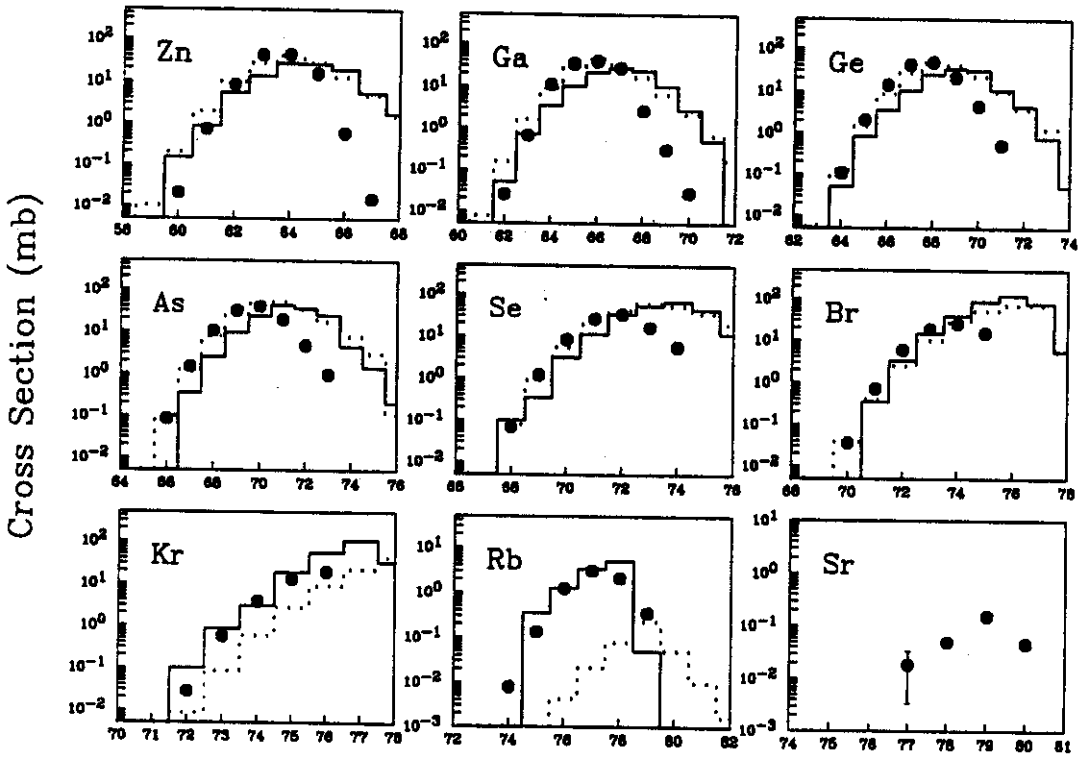

Figure 4